nature neuroscience

Disrupted-in-Schizophrenia 1 (DISC1) regulates spines of the glutamate synapse via Rac1

Akiko Hayashi-Takagi[1], Manabu Takaki[1], Nick Graziane[2], Saurav Seshadri[1], Hannah Murdoch[3], Allan J Dunlop[3], Yuichi Makino[4], Anupamaa J Seshadri[1], Koko Ishizuka[1], Deepak P Srivastava[5], Zhong Xie[5], Jay M Baraban[4], Miles D Houslay[3], Toshifumi Tomoda[6], Nicholas J Brandon[7], Atsushi Kamiya[1], Zhen Yan[2], Peter Penzes[5] & Akira Sawa[1,4]

Synaptic spines are dynamic structures that regulate neuronal responsiveness and plasticity. We examined the role of the schizophrenia risk factor DISC1 in the maintenance of spine morphology and function. We found that DISC1 anchored Kalirin-7 (Kal-7), regulating access of Kal-7 to Rac1 and controlling the duration and intensity of Rac1 activation in response to NMDA receptor activation in both cortical cultures and rat brain *in vivo*. These results explain why Rac1 and its activator (Kal-7) serve as important mediators of spine enlargement and why constitutive Rac1 activation decreases spine size. This mechanism likely underlies disturbances in glutamatergic neurotransmission that have been frequently reported in schizophrenia that can lead to alteration of dendritic spines with consequential major pathological changes in brain function. Furthermore, the concept of a signalosome involving disease-associated factors, such as DISC1 and glutamate, may well contribute to the multifactorial and polygenetic characteristics of schizophrenia.

Disturbances in neuronal connectivity, particularly in glutamatergic synaptic connections, underlie schizophrenia and associated disorders[1–3]. Neuropathological studies with autopsied brains from individuals with schizophrenia have reported reduced numbers of dendritic spines[4,5]. Morphological changes of the dendritic spine are directly correlated with its functional deficits[6,7]. Indeed, in the brains of individuals with schizophrenia, alterations of the levels of glutamate and its metabolite *N*-acetylaspartate are detected by magnetic resonance spectroscopy[8]. Furthermore, some studies have suggested that there is a reduction in glutamate receptor binding in the prefrontal cortex of individuals with schizophrenia using a selective tracer for the NMDA receptor, [^{123}I] CNS-1261, in single-photon emission tomography[9]. Consistent with these findings, molecular profiling studies on postmortem brain from individuals with schizophrenia have found decreased expression of important synaptic molecules[10], including Kal-7 and Rho-family small G-proteins[11], which are important for spine structural and functional plasticity[12,13]. This notion has been reinforced by the recent discovery of genetic susceptibility factors for schizophrenia that are enriched in the dendritic spine, including Neuregulin-1, ErbB4, RGS4 and CAPON[14,15], some of which reportedly interact with postsynaptic density 95 (PSD-95), a major structural protein of the postsynaptic density of the glutamate synapse[16,17].

DISC1 is another promising susceptibility factor for schizophrenia and related disorders, and its disruption as a result of balanced chromosomal translocation causes a familial psychosis in a large Scottish pedigree[18]. Notably, several studies have reported that common variants of DISC1 are associated with endophenotypes relevant to schizophrenia, including decreased gray-matter volume and poor working memory[19–22]. Using immunoelectron microscopy, we previously found that a pool of DISC1 is enriched in the postsynaptic density (PSD) in human brains[23]. Morphological changes of spines have been reported in an animal model in which some DISC1 isoforms are genetically deleted[24]. Here we examined a method by which DISC1 regulates synaptic spines, whereby DISC1 anchors Kal-7 in a protein complex and limits and controls access of Kal-7 to Rac1 in response to activation of the NMDA glutamate receptor.

RESULTS

DISC1 modulates structure and function of spines via Kal-7

Consistent with our histological data from human brains, we observed enrichment of DISC1 in the Triton X-100–resistant PSD fractions of adult rat brains (**Supplementary Fig. 1**). Synaptic DISC1 became prominent in mature neurons, whereas centrosomal DISC1, evident in proliferating cells and immature neurons, disappeared (**Supplementary Fig. 1**). To test possible roles for DISC1 in the PSD of mature neurons, we used RNA interference (RNAi)[25]. Two independent short-hairpin RNAs (shRNAs) knocked down both hemagglutinin (HA)-tagged full-length exogenous DISC1 (DISC1-FL) and major isoforms of endogenous DISC1 (**Supplementary Fig. 2**).

[1]Department of Psychiatry, Johns Hopkins University School of Medicine, Baltimore, Maryland, USA. [2]Department of Physiology and Biophysics, University at Buffalo, State University of New York, Buffalo, New York, USA. [3]Neuroscience and Molecular Pharmacology, Faculty of Biomedical and Life Sciences, University of Glasgow, Glasgow, UK. [4]Department of Neuroscience, Johns Hopkins University School of Medicine, Baltimore, Maryland, USA. [5]Department of Physiology, Northwestern University Feinberg School of Medicine, Chicago, Illinois, USA. [6]Beckman Research Institute of the City of Hope, Duarte, California, USA. [7]Pfizer, Princeton, New Jersey, USA. Correspondence and requests for materials should be addressed A.S. (asawa1@jhmi.edu).

Received 27 July 2009; accepted 23 December 2009; published online 7 February 2010; doi:10.1038/nn.2487

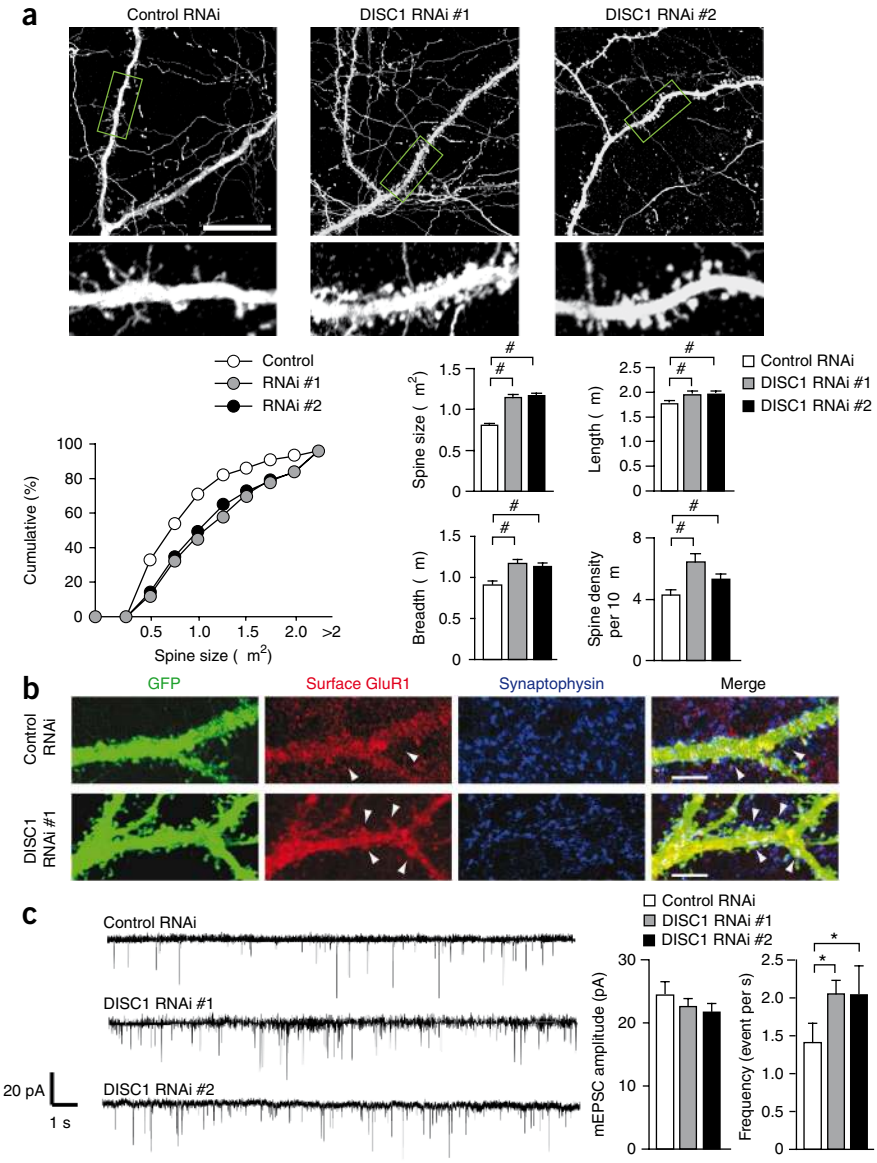

Figure 1 Short-term knockdown of DISC1 elicits spine enlargement in rat primary cortical neurons. (**a**) Spine changes in mature neurons by short-term knockdown (2 d) of DISC1 using two independent RNAi . Scale bar represents 50 μm. $^{\#}P < 0.001$. (**b**) Enhanced surface expression of GluR1 on the spine. Arrowheads indicate GluR1 clustering on spines. GFP, green fluorescent protein. (**c**) Increase in the frequency of miniature excitatory postsynaptic currents (mEPSC). Left, representative mEPSC traces. Right, mEPSC amplitude and frequency. Error bars indicate s.e.m. $^{*}P < 0.05$.

Application of DISC1 RNAi resulted in a decrease of DISC1 in postsynaptic spines (**Supplementary Fig. 3**), resulting in an increase in the size and number of spine-like structures 2 d after DISC1 RNAi application (**Fig. 1a** and **Supplementary Fig. 4**). These spine-like structures likely formed functional synapses, as indicated by increases in the surface expression of the AMPA-type glutamate receptor GluR1 (**Fig. 1b** and **Supplementary Fig. 5**), a mechanism of synaptic potentiation[26]. Increased frequency of miniature excitatory postsynaptic currents (mEPSCs) in neurons with DISC1 knockdown was observed electrophysiologically (**Fig. 1c**). To rule out the possibility of off-target effects of RNAi, we carried out quantitative real-time PCR for 2′,5′-oligoadenylate synthetase (OAS1). We found no induction of OAS1 with control or DISC1 RNAi (**Supplementary Fig. 2**). These data indicate a regulatory role for DISC1 in spines.

DISC1 interacts with many proteins, including several synaptic proteins[21,22]. Among the synaptic proteins identified as putative DISC1 partners by yeast two-hybrid screenings, Kal-7, a GDP/GTP exchange factor (GEF) for Rac1, is well known as a regulator of spine morphology and plasticity in association with neuronal activity[27]. Indeed, recent studies have shown that Kal-7 is required for proper spine formation[28,29]. As with other proteins associated with schizophrenia, Kal-7 interacts with PSD-95 (ref. 27). Thus, we hypothesized that DISC1 might regulate Kal-7 in conjunction with PSD-95. Interaction of Kal-7 and PSD-95 with DISC1 was confirmed by co-immunoprecipitation from primary cortical neurons and rat brains, particularly in the synaptosome (**Fig. 2a**). In contrast, DISC1 did not interact with other GEFs[30,31], such as Tiam-1 and βPIX (**Fig. 2a**).

To ascertain the domain of DISC1 that is critical for binding Kal-7, we first examined a variety of deletion constructs of DISC1. We found that deletion of amino acids 350–394 of DISC1 (DISC1–ΔKal-7) abolished DISC1/Kal-7 binding (**Supplementary Fig. 6**). This is consistent with yeast two-hybrid screening in which N-terminal DISC1 (amino acids 1–382) interacted with a fragment of Kal-7 (**Supplementary Fig. 6**). The binding domain(s) of DISC1 for Kal-7 were further validated by peptide array analysis, which relies on direct protein-peptide interactions[32]. We probed a scanning library of 25-mer peptides, each displaced in sequence by five amino acids and reflecting the entire sequence of DISC1, with a purified recombinant Kal-7 fragment (amino acids 588–1,137) that corresponded to the domain for DISC1 binding that was identified by co-immunoprecipitation with various Kal-7 deletion mutants (**Supplementary Fig. 6**). Peptides that contained amino acids 376–405 of DISC1 showed the strongest interaction signal with recombinant Kal-7, consistent with the data from deletion mutants and the notion that DISC1 interacts directly with Kal-7 (**Supplementary Fig. 6**). The Kal-7–binding domain on DISC1 (amino acids 350–394) is distinct from that required for interaction with cAMP phosphodiesterase-4 (PDE4) or the kinesin superfamily member KIF5 (refs. 33–35) (**Supplementary Fig. 6**).

Overexpression of DISC1-FL decreased spine size in neurons 2 d after transfection, whereas overexpression of DISC1–ΔKal-7 did not (**Fig. 2b** and **Supplementary Fig. 7**). This result is consistent with the increased spine size that we observed on knockdown of DISC1 (**Fig. 1a**). Moreover, the DISC1 RNAi–induced spine enlargement and increase in mEPSC frequency were completely normalized by the overexpression of DISC1-FL^{R} (equivalent to DISC1-FL at the amino acid level but with three nucleotide mutations) but not by that of DISC1–ΔKal-7^{R} (**Fig. 2c,d**). Knockdown of DISC1 did not, however, affect the localization of Kal-7 in the spines (**Supplementary Fig. 8**).

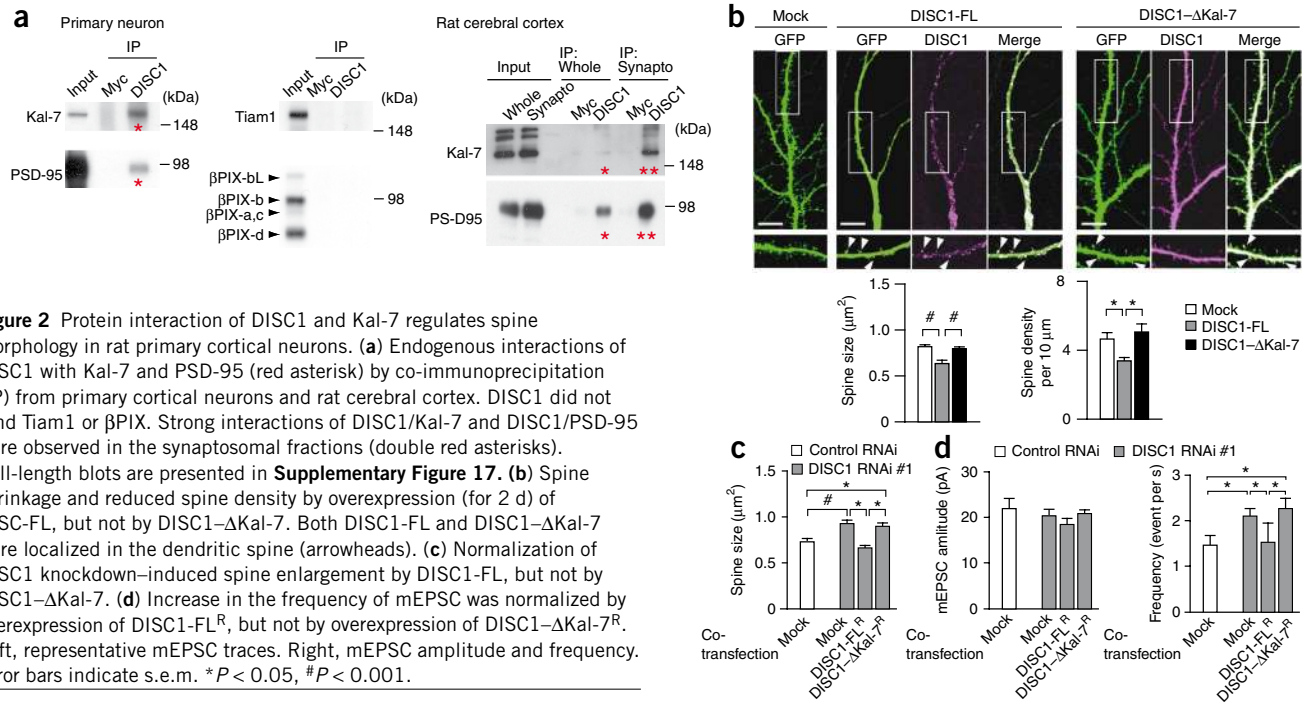

Figure 2 Protein interaction of DISC1 and Kal-7 regulates spine morphology in rat primary cortical neurons. (**a**) Endogenous interactions of DISC1 with Kal-7 and PSD-95 (red asterisk) by co-immunoprecipitation (IP) from primary cortical neurons and rat cerebral cortex. DISC1 did not bind Tiam1 or βPIX. Strong interactions of DISC1/Kal-7 and DISC1/PSD-95 were observed in the synaptosomal fractions (double red asterisks). Full-length blots are presented in **Supplementary Figure 17.** (**b**) Spine shrinkage and reduced spine density by overexpression (for 2 d) of DISC-FL, but not by DISC1–ΔKal-7. Both DISC1-FL and DISC1–ΔKal-7 were localized in the dendritic spine (arrowheads). (**c**) Normalization of DISC1 knockdown–induced spine enlargement by DISC1-FL, but not by DISC1–ΔKal-7. (**d**) Increase in the frequency of mEPSC was normalized by overexpression of DISC1-FL^R, but not by overexpression of DISC1–ΔKal-7^R. Left, representative mEPSC traces. Right, mEPSC amplitude and frequency. Error bars indicate s.e.m. $^*P < 0.05$, $^\#P < 0.001$.

These results support the notion that DISC1/Kal-7 protein interaction in the spine is crucial for regulating its morphology.

Influence of NMDAR on DISC1/Kal-7/PSD-95/Rac1 signaling

We next addressed the molecular mechanism by which DISC1 affects Kal-7 activity and, subsequently, spine morphology. Because Kal-7 binds to PSD-95 (ref. 27), we asked whether DISC1 might influence the interaction of these two proteins. In primary neurons, overexpression of DISC1-FL markedly increased the binding between Kal-7 and PSD-95, whereas overexpression of DISC1–ΔKal-7 did not (**Fig. 3a**). In contrast, knockdown of DISC1 reduced the Kal-7/PSD-95 interaction in primary cortical neuron cultures (**Fig. 3b** and **Supplementary Fig. 9**). These results suggest that DISC1 functions as a molecular signaling scaffold that augments the Kal-7–PSD-95 interaction.

The signaling of Kal-7 to Rac1 is coupled with neuronal activity via the NMDA receptor[27]. We therefore examined how neuronal activity might modulate protein interactions among Kal-7, PSD-95 and DISC1 by using electroconvulsive treatment (ECT), which elicits neuronal activation *in vivo*[36]. We observed significant decreases in protein interactions between Kal-7 and PSD-95, Kal-7 and DISC1, and DISC1 and PSD-95 in brain homogenates after ECT ($P = 0.013$, $P = 0.049$ and $P = 0.04$, respectively; **Fig.4a** and **Supplementary Fig. 9**). To confirm that these changes were the results of neuronal activation via the NMDA receptor in primary neurons, we used an established protocol in which withdrawal of amino-5-phosphonovaleric acid (AP5), a potent inhibitor of the NMDA receptor, is used to activate the receptor[27]. Dissociation of the DISC1–Kal-7–PSD-95 complex was observed on AP5 withdrawal, suggesting that the altered protein-protein interactions were dependent on activation of the NMDA receptor (**Fig. 4b** and **Supplementary Fig. 9**). Activation of Rac1 was also observed on AP5 withdrawal (**Fig. 4b**). These findings suggest that Kal-7 is released from DISC1 in an activity-dependent manner in which the resultant free Kal-7 might activate Rac1 and thereby modulate spine structure.

To validate this notion, we assessed whether Rac1 activation could be influenced by DISC1. Activation of Rac1, as determined by the level of GTP-bound Rac1, was significantly reduced by transfection of DISC1-FL ($P = 0.03$), but not DISC1–ΔKal-7, in primary neurons (**Fig. 5a**). Accordingly, DISC1 knockdown led to Rac1 activation, as detected by increased GTP-bound Rac1 and phosphorylation of p21-activated kinase (Pak1; **Fig. 5a**). Furthermore, we observed a decrease in Rac1–Kal-7 binding when DISC1-FL was overexpressed (**Fig. 5b**). This protein interaction was not changed when DISC1–ΔKal-7 was expressed in neurons. These results are consistent with the notion that DISC1 blocks Rac1 activation by inhibiting access of Kal-7 to Rac1. Stoichiometric analyses with recombinant

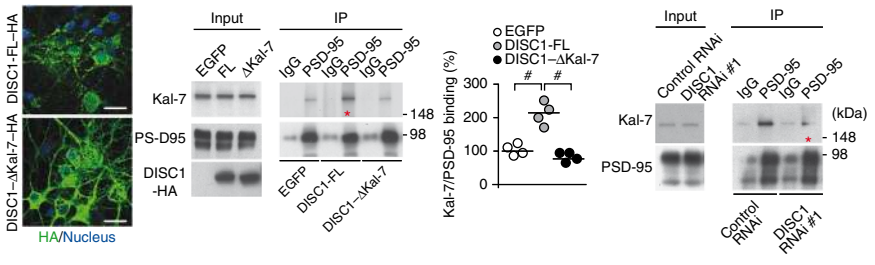

Figure 3 Augmentation of Kal-7–PSD-95 protein binding by DISC1 in rat primary cortical neurons. (**a**) Increased Kal-7–PSD-95 protein binding by overexpression of DISC1. Left, immunofluorescent cell staining indicating that the majority of neurons were infected with Sindbis virus expressing DISC1-FL–HA or DISC1–ΔKal-7–HA. Middle and right, increased binding of Kal-7 and PSD-95 by overexpression of DISC1-FL (red asterisk), but not of DISC1–ΔKal-7. Scale bars represent 20 μm. EGFP, enhanced GFP. (**b**) Decrease in Kal-7–PSD-95 binding on lentivirus-based DISC1 knockdown. $^*P < 0.05$, $^\#P < 0.001$. Full-length blots are presented in **Supplementary Figure 17**.

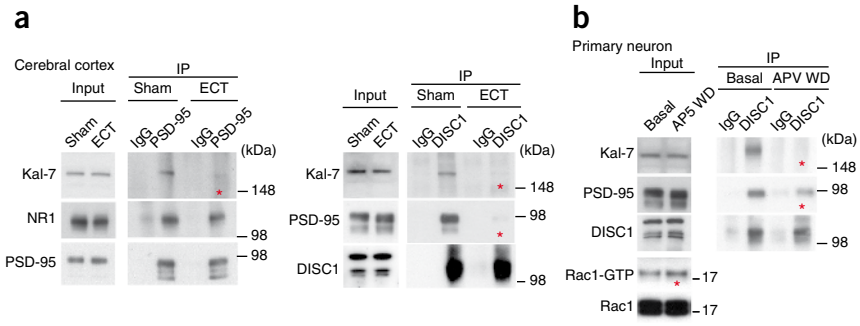

Figure 4 Protein interaction of DISC1–Kal-7–PSD-95 influenced by activation of the NMDA-type glutamate receptor. (**a**) Decrease in interactions among DISC1, Kal-7 and PSD-95 (red asterisk) 3 min after ECT in rat brains *in vivo*. Full-length blots are presented in **Supplementary Figure 18.** (**b**) Decrease in the interactions of DISC1–Kal-7 and DISC1–PSD-95 (red asterisk) as well as activation of Rac1 (input, red asterisk) after selective activation of the NMDA receptor by AP5 withdrawal (WD). $^{*}P < 0.05$. Full-length blots are presented in **Supplementary Figure 18**.

DISC1, Kal-7 and PSD-95 indicated that DISC1, as a scaffold protein, could efficiently anchor Kal-7 and PSD-95 (**Supplementary Figs. 10** and **11**). This observation is consistent with the nature of these proteins to be prone to oligomerize[37,38]. Consistent with previous reports[39], we found that Kal-7 selectively activated Rac1, but not Cdc42 and RhoA (**Supplementary Fig. 12**). The presence of a functional DISC1–Kal-7–Rac1 signalosome is also supported by our finding that DISC1 RNAi–induced spine enlargement was abolished by co-transfection with either Kal-7 RNAi (data not shown) or a dominant-negative Rac1 construct (Rac1-DN) (**Fig. 5c** and **Supplementary Fig. 13**). Together, these data suggest that Kal-7 is anchored to PSD-95 via DISC1 and that this complex is modulated dynamically by neuronal activation, which acts to regulate Rac1-mediated spine morphology.

Long-term effects of DISC1 on dendritic spines

Although activation of Rac1 initially leads to rapid spine growth, prolonged activation of Rac1 results in spine shrinkage in brains[40,41]. We examined this paradoxical action of Rac1 on spine morphology in our neuron cultures by introducing a constitutively active Rac1 (Rac1-CA) construct. We observed transient overgrowth of spines in neurons expressing Rac1-CA 1 d after transfection, as compared with neurons expressing either wild-type Rac1 or Rac1-DN. In contrast, the spine size in neurons with Rac1-CA 6 d after transfection was smaller than those in neurons expressing wild-type Rac1 or Rac1-DN (**Fig. 6a**). This result is consistent with the notion that, although Rac1 activation is crucial for rapid spine growth, its continuous activation leads to deleterious effects on spines. As DISC1 may control access of Kal-7 to Rac1, we asked whether modulation of DISC1 results in similar time-dependent effects on spines. Knockdown of DISC1 might be expected to increase continuous access of Kal-7 to Rac1, leading to a condition similar to that seen when Rac1-CA was introduced, whereas overexpression of DISC1 might be expected to decrease access of Kal-7 to Rac1, a condition similar to that resulting from Rac1-DN or Kal-7 knockdown. The knockdown effects of DISC1 RNAi by plasmid vector lasted for at least 6 d (**Supplementary Fig. 2**). As predicted, we observed that the prolonged DISC1 knockdown, which was associated with decreased PSD-95–Kal-7 binding and increased Rac1 activity (**Supplementary Fig. 14**), markedly reduced spine size in primary cortical neurons (**Fig. 6b**,**c**). Overexpression of DISC1 also resulted in reduced spine size 6 d after transfection (**Fig. 6b**). These small spines induced by continuous knockdown of DISC1 had decreased surface expression of GluR1 and reduced frequency of mEPSCs, suggesting that structural shrinkage of spines was accompanied by a functional alteration (**Fig. 6d**).

Spine deterioration by prolonged DISC1 suppression was significantly rescuedby overexpression of DISC1-FL^{R} ($P = 0.018$) but not by DISC1–ΔKal-7^{R} (**Fig. 6e**,**f**). To test the long-term effects of DISC1 suppression in brain circuitry, we first used organotypic cortical cultures. Introduction of lentivirus-based shRNA to DISC1 for 7 d resulted in smaller spines in pyramidal neurons of cortical organotypic cultures (**Fig. 7a** and **Supplementary Fig. 15**). Furthermore, robust shrinkage of synaptic spine was observed when shRNA to DISC1 was stereotaxically introduced into the medial prefrontal cortex of juvenile rats (**Fig. 7b**).

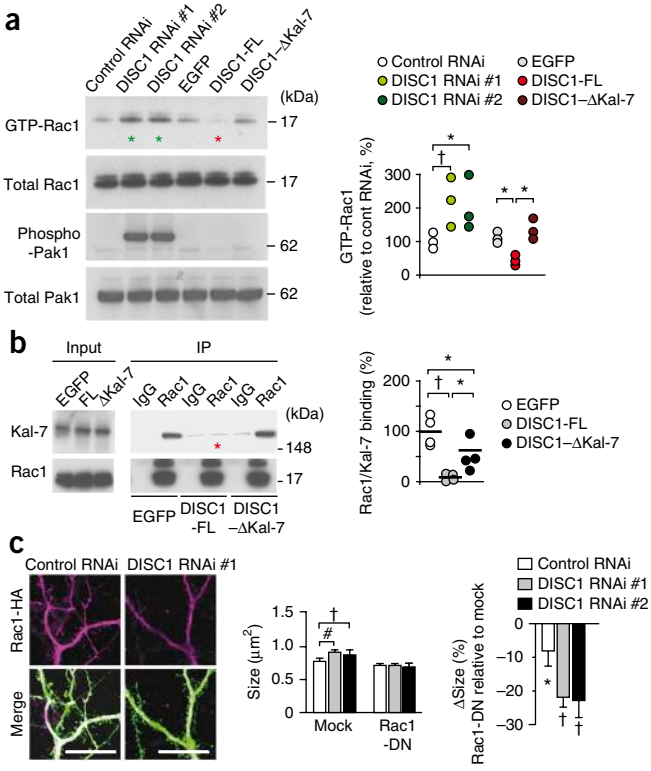

Figure 5 Regulation of Rac1 activity via signalosome of DISC1–Kal-7. (**a**) Inhibition of Rac1 activity (level of GTP-Rac1) by DISC1-FL (red asterisk), but not by DISC1–ΔKal-7, and augmentation of that activity by DISC1 knockdown (green asterisk) in primary cortical neurons. Augmented Rac1 activity was also regulated by phosphorylation of Pak1. Full-length blots are presented in **Supplementary Figure 18.** (**b**) Rac1–Kal-7 binding was reduced by DISC1-FL expression (red asterisk), but not by DISC1–ΔKal-7. (**c**) Rac1-DN expression reduced spine enlargement, indicating that Rac1 is important for DISC1 regulation of spine enlargement. Scale bars represent 20 μm. Error bars indicate s.e.m. Significant effects of Rac1-DN compared with mock are shown as $^{*}P < 0.05$, $^{\dagger}P < 0.01$ and $^{\#}P < 0.001$. Full-length blots are presented in **Supplementary Figure 18**.

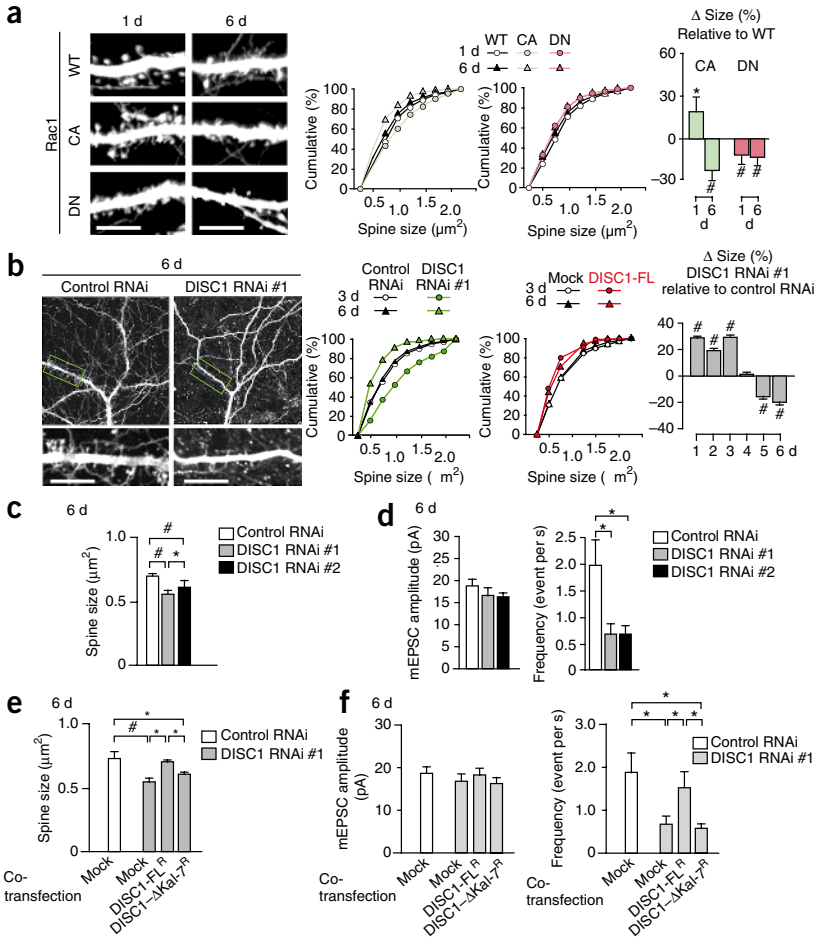

Figure 6 Long-term disturbance of DISC expression leads to spine shrinkage in rat primary cortical neurons. (**a**) Short- or long-term effect of Rac1 on spine morphology in mature neurons. Right, changes in spine size induced by expression of Rac1-CA or Rac1-DN relative to that induced by wild-type Rac1 (Rac1-WT) expression are shown (fold changes). Scale bars represent 10 μm. (**b**) Short- or long-term effect of DISC1 knockdown (green) or overexpression (red) in mature neurons. Scale bars represent 10 μm. (**c**) Reduced spine size by knockdown of DISC1 for 6 d in primary cortical culture. (**d**) Decrease in mEPSC by long-term DISC1 knockdown. (**e**) Spine deterioration (decreased spine size) induced by long-term knockdown of DISC1 was normalized by overexpression of DISC1-FL, but not by DISC1–ΔKal-7. (**f**) Spine deterioration (decreased mEPSC frequency) induced by long-term knockdown of DISC1 was normalized by overexpression of DISC1-FL, but not by DISC1–ΔKal-7. Error bars indicate s.e.m. $^{*}P < 0.05$, $^{\#}P < 0.001$.

DISCUSSION

Our results provide functional and structural insight into the role of DISC1 in dendritic spines, where DISC1 regulates Rac1 activation by confining access of Kal-7 to Rac1 (**Supplementary Fig. 16**). Although the Kal-7/Rac1 cascade is known to be an important determinant of neuronal activity–dependent spine morphological and functional plasticity[27], the mechanism underlying its regulation is not clear. Our suggest that the 'schizophrenia-related' protein DISC1 is important for mediating proper synaptic maintenance associated with neuronal activity by being closely coupled with the activation of the NMDA receptor and limiting the access of Kal-7 to Rac1 in the PSD scaffold.

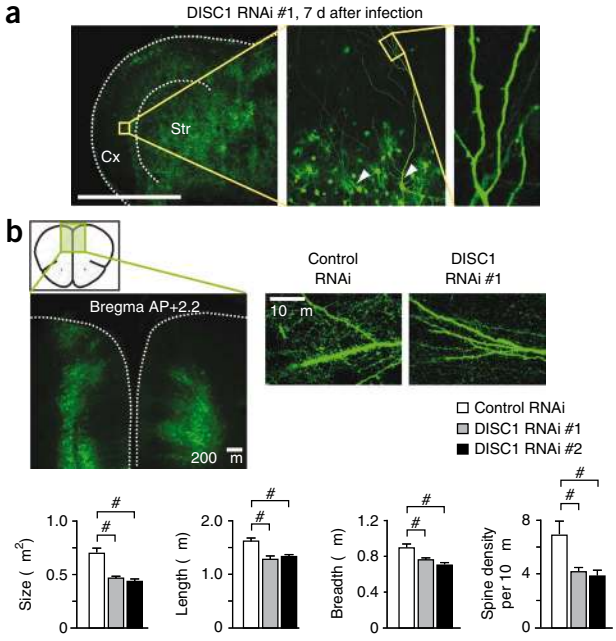

Figure 7 Long-term suppression of DISC1 leads to spine shrinkage in slices and brains *in vivo*. (**a**) Effect of long-term DISC1 knockdown on spine morphology in rat organotypic cortical culture. Representative image of culture with DISC1 RNAi (green). Scale bar represents 5 mm. Cx, cerebral cortex; Str, striatum. (**b**) Long-term effect of DISC1 knockdown on spine size in the medial prefrontal cortex. Error bars indicate s.e.m. $^{\#}P < 0.001$.

DISC1 potentially binds with proteins other than Kal-7 in the synaptic spines, such as PDE4B and KIF5 (refs. 21,22,42) (**Supplementary Fig. 6**). Nonetheless, our data support the notion that spines are regulated by DISC1–Kal-7–Rac1 in association with PSD-95, without direct involvement of the DISC1-PDE4B and DISC1-KIF5 protein cascades. It is possible that other genetic risk factors for schizophrenia that are known to interact with PSD-95, such as CAPON and ErbB4 (ref. 15), might indirectly modulate this proposed cascade for spine regulation. DISC1 is known to have many isoforms[43]. Our data, particularly the results of the rescue experiments with DISC1-FL^{R}, indicate that the full-length isoform of DISC1 is important in the Kal-7–Rac1 cascade, forming a DISC1–Kal-7–Rac1 signalosome, whose function is spatially restricted and probably focused on outputs governed by the NMDA receptor action.

Schizophrenia is believed to be associated with the disturbance of neuronal connectivity[2,3]. Many epidemiological studies have indicated that initial and major risks for the disease occur during neurodevelopment, although the onset of the disease occurs in juveniles and young adulthood[44]. Therefore, it is important to address mechanisms that can contribute to the onset of the disorders. Deficits in postnatal synaptic pruning at glutamate

synapses that occur just before the onset have been hypothesized as a potential mechanism[45]. The expression of full-length DISC1 reaches a peak at postnatal day 35 (ref. 46), when synaptic pruning is actively taking place[47]. It is therefore possible that disturbances in the DISC1–Kal-7–Rac1 signalosome–mediated synaptic maintenance may contribute to the juvenile onset of the diseases. Recent clinical studies have focused on subjects in the prodromal stages of schizophrenia and are exploring preventive medications that can block the progression of pre-psychotic conditions to full disease onset[48]. Thus, this disease etiology–associated molecular pathway that we propose through the DISC1–Kal-7–Rac1 signalosome may help in the identification of such therapeutic strategies that selectively target subjects with specific genetic risks.

METHODS

Methods and any associated references are available in the online version of the paper at http://www.nature.com/natureneuroscience/.

Note: Supplementary information is available on the Nature Neuroscience website.

ACKNOWLEDGMENTS

We thank Y. Lema and P. Talalay for help with manuscript preparation, A. Gruber, P. O'Donnell, P.F. Worley, R.L. Huganir, J.D. Rothstein, N. Shahani, H. Ujike, S. Kuroda, H. Bito and M. Nuriya for scientific discussions and J. Gogos, R.A. Cerione, H. Cline and A. Jeromin for providing us with reagents. This work was supported by grants from the US National Institutes of Health (MH-084018, MH-069853 and MH-088753 to A.S., MH-071316 to P.P., and MH-084233 and NS-048911 to Z.Y.), as well as by grants from Stanley (A.S.), Cure Huntington's Disease Initiative (A.S.), HighQ (A.S.), S & R Foundation (A.S.), RUSK (A.S.), National Alliance for Research on Schizophrenia and Depression (A.S., A.H.-T., A.K. and P.P.), National Alliance for Autism Research (P.P.), Uehara (A.H.-T. and M.T.), Medical Research Council (G0600765 to M.D.H.) and the European Union (LSHB-CT-2006-037189 to M.D.H.).

AUTHOR CONTRIBUTIONS

A.H.-T., M.T., N.G., S.S., H.M., A.J.D. and T.T. conducted the experiments. Y.M., A.J.S., K.I., D.P.S. and Z.X. provided assistance for the experiments. J.M.B., M.D.H., T.T., N.J.B., A.K., Z.Y. and P.P. contributed to experimental design. A.H.-T., M.D.H., N.J.B. and A.S. wrote the manuscript. A.S. led the overall experimental design of the entire project.

COMPETING INTERESTS STATEMENT

The authors declare no competing financial interests.

Published online at http://www.nature.com/natureneuroscience/.
Reprints and permissions information is available online at http://www.nature.com/reprintsandpermissions/.

1. Goff, D.C. & Coyle, J.T. The emerging role of glutamate in the pathophysiology and treatment of schizophrenia. *Am. J. Psychiatry* **158**, 1367–1377 (2001).
2. Moghaddam, B. Bringing order to the glutamate chaos in schizophrenia. *Neuron* **40**, 881–884 (2003).
3. McCullumsmith, R.E., Clinton, S.M. & Meador-Woodruff, J.H. Schizophrenia as a disorder of neuroplasticity. *Int. Rev. Neurobiol.* **59**, 19–45 (2004).
4. Glantz, L.A. & Lewis, D.A. Decreased dendritic spine density on prefrontal cortical pyramidal neurons in schizophrenia. *Arch. Gen. Psychiatry* **57**, 65–73 (2000).
5. Garey, L.J. *et al.* Reduced dendritic spine density on cerebral cortical pyramidal neurons in schizophrenia. *J. Neurol. Neurosurg. Psychiatry* **65**, 446–453 (1998).
6. Maletic-Savatic, M., Malinow, R. & Svoboda, K. Rapid dendritic morphogenesis in CA1 hippocampal dendrites induced by synaptic activity. *Science* **283**, 1923–1927 (1999).
7. Matsuzaki, M., Honkura, N., Ellis-Davies, G.C. & Kasai, H. Structural basis of long-term potentiation in single dendritic spines. *Nature* **429**, 761–766 (2004).
8. Steen, R.G., Hamer, R.M. & Lieberman, J.A. Measurement of brain metabolites by 1H magnetic resonance spectroscopy in patients with schizophrenia: a systematic review and meta-analysis. *Neuropsychopharmacology* **30**, 1949–1962 (2005).
9. Pilowsky, L.S. *et al.* First *in vivo* evidence of an NMDA receptor deficit in medication-free schizophrenic patients. *Mol. Psychiatry* **11**, 118–119 (2006).
10. Mirnics, K., Middleton, F.A., Lewis, D.A. & Levitt, P. Analysis of complex brain disorders with gene expression microarrays: schizophrenia as a disease of the synapse. *Trends Neurosci.* **24**, 479–486 (2001).
11. Hill, J.J., Hashimoto, T. & Lewis, D.A. Molecular mechanisms contributing to dendritic spine alterations in the prefrontal cortex of subjects with schizophrenia. *Mol. Psychiatry* **11**, 557–566 (2006).
12. Fischer, M., Kaech, S., Knutti, D. & Matus, A. Rapid actin-based plasticity in dendritic spines. *Neuron* **20**, 847–854 (1998).
13. Carlisle, H.J. & Kennedy, M.B. Spine architecture and synaptic plasticity. *Trends Neurosci.* **28**, 182–187 (2005).
14. Harrison, P.J. & West, V.A. Six degrees of separation: on the prior probability that schizophrenia susceptibility genes converge on synapses, glutamate and NMDA receptors. *Mol. Psychiatry* **11**, 981–983 (2006).
15. Hashimoto, R., Tankou, S., Takeda, M. & Sawa, A. Postsynaptic density: a key convergent site for schizophrenia susceptibility factors and possible target for drug development. *Drugs Today (Barc)* **43**, 645–654 (2007).
16. Sheng, M. & Hoogenraad, C.C. The postsynaptic architecture of excitatory synapses: a more quantitative view. *Annu. Rev. Biochem.* **76**, 823–847 (2007).
17. Blanpied, T.A., Kerr, J.M. & Ehlers, M.D. Structural plasticity with preserved topology in the postsynaptic protein network. *Proc. Natl. Acad. Sci. USA* **105**, 12587–12592 (2008).
18. St. Clair, D. *et al.* Association within a family of a balanced autosomal translocation with major mental illness. *Lancet* **336**, 13–16 (1990).
19. Callicott, J.H. *et al.* Variation in DISC1 affects hippocampal structure and function and increases risk for schizophrenia. *Proc. Natl. Acad. Sci. USA* **102**, 8627–8632 (2005).
20. Cannon, T.D. *et al.* Association of DISCC1/TRAX haplotypes with schizophrenia, reduced prefrontal gray matter, and impaired short- and long-term memory. *Arch. Gen. Psychiatry* **62**, 1205–1213 (2005).
21. Ishizuka, K., Paek, M., Kamiya, A. & Sawa, A. A review of Disrupted-In-Schizophrenia-1 (DISC1): neurodevelopment, cognition, and mental conditions. *Biol. Psychiatry* **59**, 1189–1197 (2006).
22. Chubb, J.E., Bradshaw, N.J., Soares, D.C., Porteous, D.J. & Millar, J.K. The DISC locus in psychiatric illness. *Mol. Psychiatry* **13**, 36–64 (2008).
23. Kirkpatrick, B. *et al.* DISC1 immunoreactivity at the light and ultrastructural level in the human neocortex. *J. Comp. Neurol.* **497**, 436–450 (2006).
24. Kvajo, M. *et al.* A mutation in mouse Disc1 that models a schizophrenia risk allele leads to specific alterations in neuronal architecture and cognition. *Proc. Natl. Acad. Sci. USA* **105**, 7076–7081 (2008).
25. Kamiya, A. *et al.* A schizophrenia-associated mutation of DISC1 perturbs cerebral cortex development. *Nat. Cell Biol.* **7**, 1167–1178 (2005).
26. Shi, S.H. *et al.* Rapid spine delivery and redistribution of AMPA receptors after synaptic NMDA receptor activation. *Science* **284**, 1811–1816 (1999).
27. Xie, Z. *et al.* Kalirin-7 controls activity-dependent structural and functional plasticity of dendritic spines. *Neuron* **56**, 640–656 (2007).
28. Ma, X.M., Wang, Y., Ferraro, F., Mains, R.E. & Eipper, B.A. Kalirin-7 is an essential component of both shaft and spine excitatory synapses in hippocampal interneurons. *J. Neurosci.* **28**, 711–724 (2008).
29. Cahill, M. *et al.* Kalirin regulates cortical spine morphogenesis and disease-related behavioral phenotypes. *Proc. Natl. Acad. Sci. USA* **106**, 13058–13063 (2009).
30. Saneyoshi, T. *et al.* Activity-dependent synaptogenesis: regulation by a CaM-kinase kinase/CaM-kinase I/betaPIX signaling complex. *Neuron* **57**, 94–107 (2008).
31. Tolias, K.F. *et al.* The Rac1-GEF Tiam1 couples the NMDA receptor to the activity-dependent development of dendritic arbors and spines. *Neuron* **45**, 525–538 (2005).
32. Bolger, G.B. *et al.* Scanning peptide array analyses identify overlapping binding sites for the signalling scaffold proteins, beta-arrestin and RACK1, in cAMP-specific phosphodiesterase PDE4D5. *Biochem. J.* **398**, 23–36 (2006).
33. Millar, J.K. *et al.* Drosoph. Inf. Serv.C1 and PDE4B are interacting genetic factors in schizophrenia that regulate cAMP signaling. *Science* **310**, 1187–1191 (2005).
34. Murdoch, H. *et al.* Isoform-selective susceptibility of DISC1/phosphodiesterase-4 complexes to dissociation by elevated intracellular cAMP levels. *J. Neurosci.* **27**, 9513–9524 (2007).
35. Taya, S. *et al.* DISC1 regulates the transport of the NUDEL/LIS1/14–3-3epsilon complex through kinesin-1. *J. Neurosci.* **27**, 15–26 (2007).
36. Steward, O. & Worley, P.F. Selective targeting of newly synthesized Arc mRNA to active synapses requires NMDA receptor activation. *Neuron* **30**, 227–240 (2001).
37. Hsueh, Y.P., Kim, E. & Sheng, M. Disulfide-linked head-to-head multimerization in the mechanism of ion channel clustering by PSD-95. *Neuron* **18**, 803–814 (1997).
38. Djinovic-Carugo, K., Gautel, M., Ylanne, J. & Young, P. The spectrin repeat: a structural platform for cytoskeletal protein assemblies. *FEBS Lett.* **513**, 119–123 (2002).
39. Rabiner, C.A., Mains, R.E. & Eipper, B.A. Kalirin: a dual Rho guanine nucleotide exchange factor that is so much more than the sum of its many parts. *Neuroscientist* **11**, 148–160 (2005).
40. Luo, L. *et al.* Differential effects of the Rac GTPase on Purkinje cell axons and dendritic trunks and spines. *Nature* **379**, 837–840 (1996).
41. Tashiro, A., Minden, A. & Yuste, R. Regulation of dendritic spine morphology by the rho family of small GTPases: antagonistic roles of Rac and Rho. *Cereb. Cortex* **10**, 927–938 (2000).
42. Camargo, L.M. *et al.* Disrupted in Schizophrenia 1 interactome: evidence for the close connectivity of risk genes and a potential synaptic basis for schizophrenia. *Mol. Psychiatry* **12**, 74–86 (2007).
43. Ishizuka, K. *et al.* Evidence that many of the DISC1 isoforms in C57BL/6J mice are also expressed in 129S6/SvEv mice. *Mol. Psychiatry* **12**, 897–899 (2007).
44. Jaaro-Peled, H. *et al.* Neurodevelopmental mechanisms of schizophrenia: understanding disturbed postnatal brain maturation through Neuregulin-1 and DISC1. *Trends Neurosci.* **32**, 485–495 (2009).
45. McGlashan, T.H. & Hoffman, R.E. Schizophrenia as a disorder of developmentally reduced synaptic connectivity. *Arch. Gen. Psychiatry* **57**, 637–648 (2000).
46. Schurov, I.L., Handford, E.J., Brandon, N.J. & Whiting, P.J. Expression of disrupted in schizophrenia 1 (DISC1) protein in the adult and developing mouse brain indicates its role in neurodevelopment. *Mol. Psychiatry* **9**, 1100–1110 (2004).
47. Holtmaat, A.J. *et al.* Transient and persistent dendritic spines in the neocortex *in vivo*. *Neuron* **45**, 279–291 (2005).
48. McGlashan, T.H. & Johannessen, J.O. Early detection and intervention with schizophrenia: rationale. *Schizophr. Bull.* **22**, 201–222 (1996).

ONLINE METHODS

Antibodies. The N-terminal polyclonal antibody to DISC1 was a generous gift from J. Gogos (Columbia University)[49]. Additional DISC1, Kal-7–specific and Kal-spectrin antibodies were described previously[25,27]. Antibodies to Myc (Santa Cruz Biotechnology), PSD-95 (NeuroMab), synaptophysin (Sigma-Aldrich), KIF5 (Millipore), GFP (Invitrogen), HA (Covances), phospho-Pak1 (Cell Signaling Technology), Pak1 (Cell Signaling Technology), Tiam1 (Santa Cruz), GluR1(Millipore), βPIX (Millipore) and Alexa 405–, 488–, 568– or 633–conjugated secondary antibodies (Invitrogen) were used.

Plasmid construction and transfection. Cloning, mutagenesis and deletion of DISC1 and Kal-7 were conducted as described previously[25]. Rac1-WT, Rac1-CA (G12V) and Rac1-DN (T17N) were from Missouri University of Science and Technology. H1-RNA polymerase III promoter–driven shRNAs to DISC1 (#1 with strong effect and #2 with weaker effect), which also carry EGFP under the control of the CMV promoter, were previously described[25]. Cultured cells were transfected with plasmids using of Lipofectamine2000 (Invitrogen). In primary neuron cultures, we transfected 2 μg of pSuper-Venus RNAi into 1.5×10^5 cells. For 293 cells, 2 μg of pRK/DISC1-HA expression construct and 2 μg of pSuper-Venus RNAi construct were transfected (at 90% confluence in an 18-mm dish). In standard analyses, primary neurons were transfected after 23 d *in vitro* and maintained for 1–6 d after transfection.

Recombinant proteins tagged with GST or MBP. The full-length mouse DISC1 cDNA was cloned in pMAL vector for DISC1-MBP. Likewise, full-length PSD-95 and Kal-7 (amino acid 588–1,571) were cloned into pGEX to make PSD-95–GST and Kal-7–GST, respectively. The expression plasmids were introduced into *E. coli* BL21 and grown at 23 °C with 0.1 mM isopropyl β-D-1-thiogalactopyranoside. Recombinant proteins were purified from *E. coli* with glutathione sepharose or amylose beads. Further purification was conducted with a centrifugal filter device (Amicon Ultra-100k, Millipore), with degraded protein fragments of less than 100 kDa being removed.

Viral production and infection. Lentivirus was produced by co-transfection of RNAi-containing FUGW lentiviral constructs and the helper constructs VSVG and Δ8.9 into 293FT packaging cells. Media were collected 48 h after transfection and virus was concentrated by ultracentrifugation at 25,000 *g* for 90 min. For synthesis of Sindbis virus, recombinant RNAs from Sindbis vector pSin-Rep5 (nsP2) and the packaging construct DH(26)S were generated by *in vitro* transcription using the mMESSAGE mMACHINE kit (Ambion). These RNAs were transferred into BHK cells using the GenePulser XCell system (BioRad) and media was collected after 24 h. Viral titers were calculated by counting the number of EGFP-positive cells that were present after infecting with serial dilutions of the viral solution. For infection into a primary neuron, virus solution was added to the medium (3.5×10^5 units to1.5×10^5 cells), which was changed 24 h after infection, followed by incubation for 3–7 d to allow gene knockdown. For infection of slice cultures, 1 μl of 1.8×10^5 units per μl solution was added directly to the slice. The morphology of infected cells was depicted by the fluorescence of EGFP carried in the viral vector.

Neuron cultures and treatment. All procedures related to animals were approved by the Johns Hopkins University Animal Care and Use Committee. Dissociated cortical neuron cultures from Sprague-Dawley rats were prepared as described previously[25]. Withdrawal of AP5 (Ascent Scientific) was used for chemical activation of NMDA receptor. Briefly, 200 μM AP5 was added to the culture dish 5 d after plating and was maintained in the medium with AP5. To induce AP5 withdrawal, we preincubated cells in artificial cerebrospinal fluid (ACSF; 125 mM NaCl, 2.5 mM KCl, 26.2 mM $NaHCO_3$, 1 mM NaH_2PO_4, 11 mM glucose, 5 mM HEPES, 2.5 mM $CaCl_2$ and 1.25 mM $MgCl_2$) with 200 μM AP5 for 30 min at 37 °C. Coverslips were then washed in withdrawal medium (ACSF with 30 μM D-serine, 100 μM picrotoxin and 1 μM strychnine) and transferred into new withdrawal medium for 20 min. Cells were then immediately fixed for immunofluorescence or lysed with lysis buffer for biochemical analysis such as Rac1 assay and co-immunoprecipitation (see below). Organotypic cortical cultures were prepared from cerebral cortex of postnatal day 3 (P3) pups using a McIlwain-type tissue chopper. A slice (400 μm thickness) was maintained on the Organotypic cell culture insert (Millipore), which consists of porous and transparent membranes, with neurobasal-N1 medium (Neurobasal medium (Invitrogen) supplemented with 2 mM L-glutamine, 5% horse serum (vol/vol), and N1 supplement (Sigma)).

Electrophysiological recordings. Recording for miniature excitatory post-synaptic currents (mEPSC) in cultured neurons ($n = 6$–12 in each group) were prepared as described previously[50]. Patch electrodes (3–5 MΩ) were filled with internal solution (130 mM cesium methanesulfate, 10 mM CsCl, 4 mM NaCl, 1 mM $MgCl_2$, 5 mM EGTA, 10 mM HEPES, 5 mM MgATP, 0.5 mM Na_2GTP, 12 mM phosphocreatine, 20 mM leupeptin and 1 mM QX314; pH 7.2–7.3, 265–270 mosm l^{-1}). The external solution consisted of 127 mM NaCl, 5 mM KCl, 2 mM $MgCl_2$, 2 mM $CaCl_2$, 12 mM glucose, 10 mM HEPES and 0.5 mM tetrodotoxin (pH 7.4, 300 mosm l^{-1}). Bicuculline (10 μM) was added to the external solution to block $GABA_A$ receptors. Recordings were obtained with an Axon Instruments 200B patch clamp amplifier that was controlled and monitored with an IBM PC running pCLAMP with a DigiData 1320 series interface (Axon Instruments). Electrode resistances in the bath were typically 2–4 MΩ. After seal rupture, series resistance (4–10 MΩ) was compensated (70–90%) and periodically monitored. The cell membrane potential was held at –70 mV. The Mini Analysis Program (Synaptosoft) was used to analyze synaptic activity. For each different condition, mEPSC recordings of 8 min were used for analysis.

Immunofluorescence cell staining. Cells were fixed with 4% formaldehyde (vol/vol) for 30 min at 25 °C. Experimental details for cell staining were as described previously[25]. For staining of surface GluR1 on the plasma membrane, fixed cells were incubated with a primary antibody to an extracellular region of GluR1 before permeabilization with Perm/Blocking buffer (2.5% normal goat serum (vol/vol) in phosphate-buffered saline (PBS) with 0.1% Triton X-100 (vol/vol)). Permeabilized cells were then stained for synaptophysin. For free-floating immunofluorescence staining of organotypic slice, the slices were fixed with 4% formaldehyde for 1 h at 25 °C, followed by permeabilization with Perm/Blocking buffer (2.5% normal goat serum in PBS with 0.3% Triton X-100) for 1 h at 25 °C. The slices were incubated for 48 h at 4 °C with a primary antibody in Perm/Blocking buffer. After rinsing with PBS (8 times, 5 min each), sections were stained with corresponding secondary antibody, followed by mounting. Cell staining was examined with a confocal microscope (LSM 510-Meta, Zeiss).

Quantitative morphological analysis of spine. Staining with antibody to GFP was used to circumvent potential unevenness of GFP diffusion in spines. For co-transfection experiments, the neurons that were clearly transfected with both GFP and the gene of interest were captured as images. Images were taken by a Zeiss LSM510-Meta with the 63× oil-immersion objective as *z* series of 6–12 images taken at 0.3-μm intervals (scan averaged, four times; 1,024 × 1,024 pixel resolution; a scan speed of 1.6 ms per pixel). The acquisition parameters were kept constant for all scans in the same experiment. Only the first dendrites that were arborized from a typical apical dendrite of the authentic pyramidal neuron with triangle cell body were subjected to morphological analysis, as previously described[27]. Two-dimensional projection reconstructions of *z* series of images, morphometric analysis and quantification were carried out using MetaMorph software version 7.1 (MDS Analytical Technologies). Individual spines on dendrites were manually traced and the area (size), maximum length (length) and head width (Breadth) of each spine was measured. Based on the sensitivity of this quantitative morphological analysis, which has been already established[27], we did not consider structures that had an area of less than 0.25 μm^2 as being a spine, as these approached the limit of resolution of our microscope. In each experiment, about 500–1,000 spines from 30–45 dendrites derived from 10–15 neurons were analyzed per condition. At least two independent analyses, mostly three, were carried out while blinded to transfection condition until statistical analysis had been done.

Preparation of synaptosomes and postsynaptic densities. Cerebral cortex dissected from adult Sprague-Dawley rats was homogenized in ten volumes of buffer A (0.32 M sucrose, 1 mM $NaHCO_3$, 1 mM $MgCl_2$ and 0.5 mM $CaCl_2$). Crude synaptosomal and postsynaptic densities were purified using the classical sucrose gradient protocol previously described[27].

Immunoprecipitation. Cells or tissue were lysed in lysis buffer (150 mM NaCl, 50 mM Tris·HCl (pH 7.4), 0.1% NP-40 and protein inhibitor cocktail (Complete,

Roche Diagnostics)). Lysates were sonicated, cell debris was cleared by centrifugation and the soluble fraction was subjected to immunoprecipitation, followed by immunoblotting. Normal IgG and antibody to Myc were used as negative controls for immunoprecipitation. The signal intensity of each band (the net signal was obtained after the subtraction of background signal obtained from the region adjacent to the band) was measured by ImageJ software (US National Institutes of Health).

Rac activation assay. Activation of Rac1 was measured with the Rac1 activity assay kit (Upstate Biotechnology) according to manufacturer's instructions. Briefly, a fusion protein consisting of the p21-binding domain of Pak1, which specifically binds to the active form of Rac1 (Rac-GTP), but not to the inactive form of Rac1 (Rac-GDP), was used for precipitation of Rac-GTP. GTP-γs and GDP were used as positive and negative controls, respectively. Phosphorylation of Pak1, a substrate for Rac1, was also used as an indicator for Rac1 activity, as binding of Rac1-GTP to Pak1 induces the autophosphorylation and activation of Pak1.

Intracerebral injections of lentiviral vectors. Sprague-Dawley rats, aged at P21–24, were anesthetized with ketamine and xylazine and placed in a stereotaxic frame to secure the cranium. An incision was made in the scalp and a hole was drilled in the skull at the desired site of injection. The location of the injection site in the prefrontal cortex was standardized among rats by using stereotaxic coordinates (anteroposterior = +2.2, mediolateral = +1.0, dorsoventral = +1.0) from the skull. A total of eight rats (four for DISC1 RNAi, four for scrambled RNAi) were bilaterally injected with 3 μl of the lentiviral preparations (1.8×10^5 unit μl^{-1}) into the medial prefrontal cortex (by using a Hamilton syringe, 0.15 μl min^{-1}). The rats were killed 8 d after injection and their brains were perfusion-fixed in 4% paraformaldehyde for subsequent immunohistochemical analysis. The morphology of infected cells was depicted by the fluorescence of EGFP carried in the viral vector.

ECT. ECT were induced in an unanesthetized Sprague-Dawley rat at P21 by delivering alternating current (current, 90 mA; frequency, 100 Hz; pulse width, 0.5 ms; shock duration, 1.0 s) via ear clip electrodes as described[36]. For biochemical analysis, animals were killed by cervical fracture, followed by dissection of cerebral cortex 3 min after electroconvulsion.

Statistics. For determination of the statistical significance between two groups, either the Student's *t* test (equal variances) or Mann Whitney U tests (unequal variances) were employed. The result of the *F* test was used to decide which test was appropriate. To compare three or more groups, we used one-way ANOVAs, followed by Dunnett-T3 *post hoc* for multiple comparisons. Statistical analyses were performed using SPSS 11.0 software (SPSS). Cross bars across scattered plots indicate the mean of all values.

49. Koike, H., Arguello, P.A., Kvajo, M., Karayiorgou, M. & Gogos, J.A. Disc1 is mutated in the 129S6/SvEv strain and modulates working memory in mice. *Proc. Natl. Acad. Sci. USA* **103**, 3693–3697 (2006).
50. Cai, X., Gu, Z., Zhong, P., Ren, Y. & Yan, Z. Serotonin 5-HT1A receptors regulate AMPA receptor channels through inhibiting Ca^{2+}/calmodulin-dependent kinase II in prefrontal cortical pyramidal neurons. *J. Biol. Chem.* **277**, 36553–36562.

doi:10.1038/nn.2487